J|A|C|S COMMUNICATIONS

Published on Web 08/24/2009

Texture of Lipid Bilayer Domains

Uffe Bernchou,[†] Jonathan Brewer,[‡] Henrik S. Midtiby,[†] John. H. Ipsen,[†] Luis A. Bagatolli,[‡] and Adam C. Simonsen*,[†]

Department of Physics and Chemistry and Department of Biochemistry and Molecular Biology, MEMPHYS − Center for Biomembrane Physics, University of Southern Denmark, Campusvej 55, DK-5230 Odense M, Denmark

Received April 27, 2009; E-mail: adam@memphys.sdu.dk

Lipid bilayers constituting the structural backbone of biomembranes may exist in a multitude of phase states each with different types of order. Characterization of model membrane domains provides a reference for domains in biomembranes formulated in the language of soft condensed matter theory. Questions related to size and composition of liquid-ordered membrane domains have attracted much interest,[1−3] but a possible texture in gel domains has so far not been examined. The corrugated substructure of ripple phase domains has been examined with AFM.[4] Here we show that polarization two-photon fluorescence microscopy (P2FM) reveals a texture of gel (g) domains which is hidden in conventional fluorescence microscopy. The gel domains are shown to be composed of subdomains each having different orientations of the tilted lipid acyl chains but having the same phase state. Image analysis of polarization scans allows the magnitude and orientation of the tilt to be spatially resolved. We observe vortex patterns which are centered at point disclinations in the domain core. Textures of the same type have historically been associated with the presence of hexatic order in Langmuir monolayers. The hexatic phase has long-range orientation order and short-range positional order. Our results indicate that hexatic order may persist in lipid bilayers and can possibly rationalize the texture we observe in gel domains.

Binary mixtures of phospholipids with different acyl chain lengths or degrees of saturation are known to phase separate into gel (g) and liquid disordered (ld) phases.[5,6] We have recently investigated domain shapes.[7] X-ray studies have shown that, in the (g) phase, the lipids have fully stretched acyl chains that are tilted with an angle ρ with respect to the unit vector **n** perpendicular to the bilayer plane.[8] Such domains have been observed in giant unilamellar vesicles (GUVs)[1] and supported bilayers[9] with a range of microscopy techniques.

We use P2FM to reveal the texture of gel domains in supported bilayers composed of a 1:1 mixture of 1,2-dioleoyl-*sn*-glycero-3-phosphocholine (DOPC) and 1,2-dipalmitoyl-*sn*-glycero-3-phosphocholine (DPPC) and labeled with the lipid probe Laurdan. Laurdan partitions equally into the gel and fluid phases but shows a membrane-phase-dependent emission spectral shift, useful for discriminating between membrane phases. The electronic transition moment **p** of Laurdan is aligned parallel to the acyl chains as sketched in Figure 1A.[10] This means that a regional difference in lipid tilt of a gel domain can be monitored as an intensity difference in the fluorescence image because the two-photon fluorescence emission varies as $\propto \cos^4$ to the angle between the electric field of the excitation light **E** and **p**.[11] By rotating the direction of linearly polarized excitation light, we can vary the azimuth angle φ between **E** and **p** and thus also the projection of **p** on the bilayer plane, the molecular director **c** (see Figure 1B). By mapping the angular intensity variation, we can establish the spatial variation of the director within single domains, i.e., the domain texture.

The presence of (ld) and (g) phases is established using the emission spectrum of Laurdan which is sensitive to the water dipolar relaxation

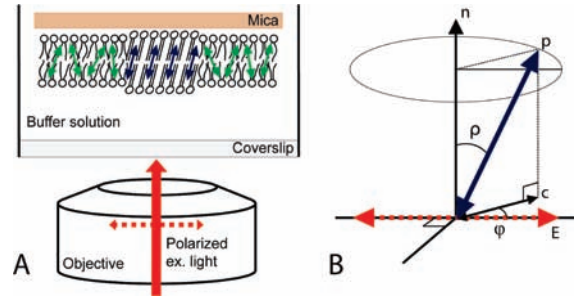

Figure 1. Schematic drawing of the experimental configuration. Laurdan is indicated with a blue arrow.

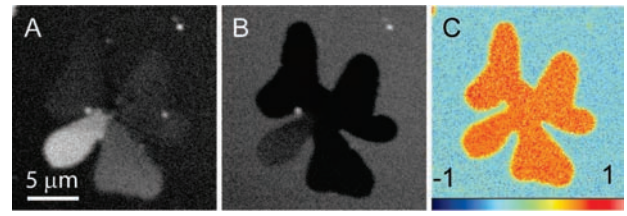

Figure 2. Images of a gel domain taken using linearly polarized excitation light and emitted light collected simultaneously in the blue- (A) and red-shifted (B) channels. The LGP image (C) constructed from the images in (A) and (B).

processes. The emission of Laurdan is blue-shifted in the gel phase and red-shifted in the liquid phase. Figure 2 shows typical Laurdan fluorescence images of the domain pattern in a DOPC/DPPC (1:1) membrane at 20 °C. Figure 2A and 2B were acquired using linearly polarized excitation light and emitted light collected simultaneously in the blue- and red-shifted channels, respectively. In Figure 2C these images have been combined to the Laurdan Generalized Polarization (LGP) image as described in detail previously.[12] The LGP function, despite its name, does not involve the polarization state of light but only the wavelength shift of emitted light. High pixel intensity in the LGP image corresponds to membrane regions with a solid character, whereas low pixel values correspond to a liquid character. From Figure 2C it is clear that the probe experiences only two different environments, namely the gel phase (g) flower shaped domain and the liquid phase (ld) surroundings. The LGP values are -0.26 ± 0.02 and 0.57 ± 0.02 for the liquid and gel phase, respectively. These values are in agreement with those reported for Giant Unilamellar Vesicles (GUVs) composed of equivalent binary mixtures.[13] The crucial observation of Figure (2C) is that the LGP value and hence the phase state are uniform within the gel domain region. This is in contrast to the orientation of the probe dipole that does vary, as shown below. The integration of P2FM and LGP allows discrimination between structural texture within one phase and different membrane phases.

We now explore how the molecular director varies within single gel domains. This is probed by variation of the linear polarization angle

[†] Department of Physics and Chemistry.
[‡] Department of Biochemistry and Molecular Biology.

10.1021/ja903375m CCC: $40.75

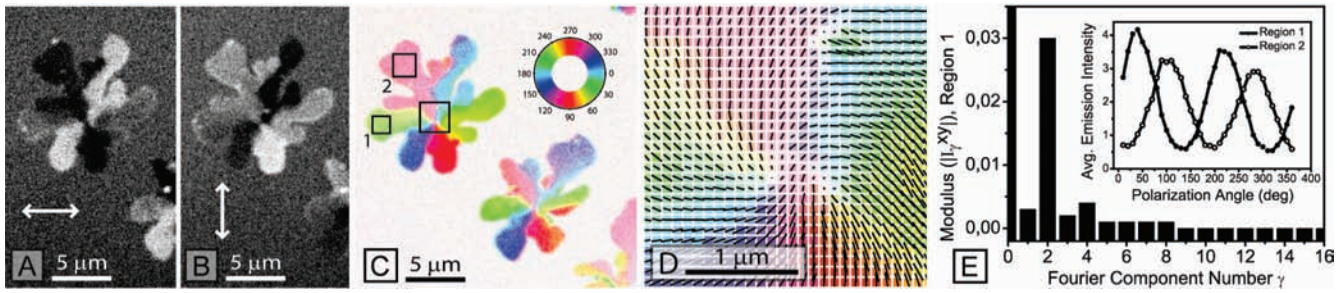

Figure 3. Sample P2FM images of gel domains (A,B) corresponding to two perpendicular angles of the electric field, as indicated by the arrows. Based on the variations in emission intensity with respect to polarization angle, a map of the subdomains is constructed (C). The orientation of the molecular director **c** has been color coded according to the insert in (C). The zoom (D) shows the central section of the domain in (C). The length of the line segments in (D) is given by the modulus $|\tilde{I}_2^{xy}|$ of the Fourier component and is proportional to the length of the molecular director. Summed emission intensities (E, insert) for pixels inside the squares marked 1 and 2 of (C). The modulus of the Fourier components for region 1, $|\tilde{I}_\gamma^{xy}|$, is shown in (E). The angle independent mode ($\gamma = 0$) has been truncated for clarity.

of the incoming excitation light. We obtain an image stack constituting a 360° rotation of the polarization direction (see movie in the Supporting Information). Figure 3A and 3B show two images from this stack taken with orthogonal polarizations. Based on intensity variations within single domains, distinct subdomains can be identified. The number of domains recorded in each experiment is typically around 20, and the number of subdomains within each domain is a narrow distribution centered around 6. Most of the subdomains share a common point in the domain center. It is convenient to analyze the angle variations in terms of the discrete Fourier transform of the pixel intensities. We denote the intensity variation of a single pixel $I_n^{xy}(n\Delta\varphi)$ with n being an integer. The complex valued discrete Fourier transform of the pixel with indices x and y is

$$\tilde{I}_n^{xy} = \frac{1}{N}\sum_{n=0}^{N-1} I_n^{xy} \exp\left(-i2\pi\frac{\gamma n}{N}\right) \quad (1)$$

with $N = 36$ in our case. Due to the nature of the angle variation, certain Fourier components γ will dominate. Intensity variations that follow the $\cos^4$ dependence will have a periodicity of 180° and have the dominant component $\tilde{I}_2^{xy}$ with $\tilde{I}_4^{xy}$ being a smaller overtone. Given the $\cos^4$ dependence, the relative magnitude of these two Fourier components is constant and it is sufficient to consider the principal one $\tilde{I}_2^{xy}$. The modulus $|\tilde{I}_2^{xy}|$ is a measure of the strength of the angular response corresponding to the length of the molecular director **c**. The argument $^1/_2 \arg(\tilde{I}_2^{xy})$ gives the dominant orientation angle of lipids within the pixel xy. Figure 3E (insert) shows the summed intensity variations of two selected regions denoted region 1 and 2. The curves show harmonic angle dependence, and the two curves are phase shifted at an angle corresponding to the change in the orientation of the molecular director between these subdomains. The Fourier analysis has been performed at the single pixel level. This generates a spatial map of the orientation and magnitude of the molecular director **c** (see Figure 3C and 3D). In Figure 3C, the variation in lipid orientation within the gel domain is color coded. The domain has a polycrystalline texture with a spatially varying director. The director is approximately parallel inside each of the subdomains indicated in Figure 3C confirming that the subdomains correspond to different orientations (φ). Figure 3D shows a zoom of the indicated square region in 3C with variations in the texture at the intersection point between the subdomains. A characteristic vortex structure is revealed in the center of the gel domain where the director is curled around a point disclination. The zoom in 3D also demonstrates some variation in the modulus $|\tilde{I}_2^{xy}|$ corresponding to a spatially varying length of the molecular director. This implies that not only the molecular tilt direction φ but also the tilt angle ρ varies among the subdomains.

Liquid condensed (LC) domains can coexist with the liquid expanded (LE) phase in Langmuir monolayers.[14,15] Such domains may contain six defect lines going radially from the center to the LC/LE interface.[16,17] The domains have been linked with hexatic order through X-ray diffraction measurements.[18] Various hexatic phases with long-range bond orientation order and short-range positional order are abundant in lipid monolayers, including phospholipids, corresponding to different couplings between the bond orientation and chain tilt degrees of freedoms.[14] The observed textures and domains shapes are also partially understood theoretically in terms of phenomenological descriptions of these modes.[19] We have shown that similar textures and domain morphologies are possible in lipid bilayers, thus providing some support for the notion that hexatic order can persist in bilayers. A definitive identification of the phase state would require complementary scattering measurements which can reveal the range of positional order (see Supporting Information for a further discussion). The results point to a possible increased complexity of biomembranes associated with an inhomogeneous internal structure of condensed domains.

Acknowledgment. The Danish National Research Foundation is acknowledged for support via a grant to MEMPHYS.

Supporting Information Available: Experimental details. Discussion of hexatic order and domain texture. Movie and raw image data of figure 3. This material is available free of charge via the Internet at http://pubs.acs.org.

References

(1) Bagatolli, L. A. *Biochim. Biophys. Acta* **2006**, *1758*, 1541–1556.
(2) London, E. *Biochim. Biophys. Acta* **2005**, *1746*, 203–220.
(3) Veatch, S. L.; Keller, S. L. *Biochim. Biophys. Acta* **2005**, *1746*, 172–185.
(4) Kaasgaard, T.; Leidy, C.; Crowe, J. H.; Mouritsen, O. G.; Jorgensen, K. *Biophys. J.* **2003**, *85*, 350–360.
(5) Seeger, H. M.; Fidorra, M.; Heimburg, T. *Macromol. Symp.* **2004**, *219*, 85–96.
(6) Sankaram, M. B.; Thompson, T. E. *Biochemistry* **1992**, *31*, 8258–8268.
(7) Bernchou, U.; Ipsen, J. H.; Simonsen, A. C. *J. Phys. Chem. B* **2009**, *113*, 7170–7177.
(8) Nagle, J. F.; Tristram-Nagle, S. *Biochim. Biophys. Acta* **2000**, *1469*, 159–195.
(9) Blanchette, C. D.; Orme, C. A.; Ratto, T. V.; Longo, M. L. *Langmuir* **2008**, *24*, 1219–1224.
(10) Bagatolli, L. A.; Gratton, E. *Biophys. J.* **1999**, *77*, 2090–2101.
(11) Bopp, M. A.; Jia, Y.; Haran, G.; Morlino, E. A.; Hochstrasser, R. M. *Appl. Phys. Lett.* **1998**, *73*, 7–9.
(12) Parasassi, T.; Gratton, E.; Yu, W. M.; Wilson, P.; Levi, M. *Biophys. J.* **1997**, *72*, 2413–2429.
(13) Bagatolli, L. A.; Gratton, E. *Biophys. J.* **2000**, *79*, 434–447.
(14) Kaganer, V. M.; Mohwald, H.; Dutta, P. *Rev. Mod. Phys.* **1999**, *71*, 779–819.
(15) Knobler, C. M.; Desai, R. C. *Annu. Rev. Phys. Chem.* **1992**, *43*, 207–236.
(16) Nandi, N.; Vollhardt, D. *Thin Solid Films* **2003**, *433*, 12–21.
(17) Ignes-Mullol, J.; Claret, J.; Sagues, F. *J. Phys. Chem. B* **2004**, *108*, 612–619.
(18) Kjaer, K.; Als-Nielsen, J.; Helm, C. A.; Laxhuber, L. A.; Mohwald, H. *Phys. Rev. Lett.* **1987**, *58*, 2224–2227.
(19) Fischer, T. M.; Bruinsma, R. F.; Knobler, C. M. *Phys. Rev. E* **1994**, *50*, 413–428.

JA903375M